LJMU Research Online

Aina, OS, Adams, LA, Bello, AJ and Familoni, OB

 Plasmodium falciparum histoaspartic protease inhibitor: Toxicity investigation and docking study of 2-(2-benzoyl-4-methylphenoxy) quinoline-3-carbaldehyde derivatives

http://researchonline.ljmu.ac.uk/id/eprint/26143/

Article

ORIGINAL RESEARCH ARTICLE

Plasmodium falciparum histoaspartic protease inhibitor: Toxicity investigation and docking study of 2-(2-benzoyl-4-methylphenoxy) quinoline-3-carbaldehyde derivatives

Oluwafemi S. Aina[1], Luqman A. Adams[1], Adebayo J. Bello[2], and Oluwole B. Familoni[1]*

[1]Drug Design Research Group, Department of Chemistry, University of Lagos, Lagos State, Nigeria

[2]Department of Chemistry and Biology, Redemeer's University, Osun State, Nigeria

*Corresponding author:
Oluwole B. Familoni
(familonio@unilag.edu.ng)

Abstract

Aspartic proteases can hydrolyze peptide bonds, making them potential targets for drug development against malaria parasites. In particular, inhibiting the histoaspartic protease (HAP) can disrupt the growth phase of *Plasmodium falciparum* and its ability to degrade hemoglobin for protein synthesis. Compound 5, specifically designed as 2-(2-benzoyl-4-methylphenoxy)quinoline-3-carbaldehyde, served as the basis for designing 50 hypothetical compounds (A1-A50). These compounds were subjected to *in silico* screening to assess their toxicity profiles, pharmacokinetics, bioactivity scores, and theoretical binding affinities, as a part of the drug design protocol. Out of the 50 compounds, nine lead candidates showed no toxicity to human cells. In addition, ten standard reference antimalarial drugs were included in this study for comparison. The highest binding energies were observed for compound A5 (−11.2 kcal/mol) and A31 (−11.3 kcal/mol), surpassing the performance of mefloquine, the best reference drug, which ranked ninth with a binding energy of (−9.6 kcal/mol). Compound A31 did not exhibit the evidence of interaction with either Asp215 or His32, whereas compound A5 displayed π-π stacking interactions with His_{32}. Mefloquine also did not show any interaction with Asp215 or His32. Moreover, compound A5 demonstrated greater hydrophobic interactions at the active site with most binding residues, except for Lys_7 in the hydrophobic region. This characteristic suggests that compound A5 may have the ability to adopt a smaller surface area, exhibit increased biological activity, and have reduced interactions with water, which could facilitate slower clearance. Based on the assessment of various drug-likeness parameters, compound A5 (2-(2-benzoyl-4-methylphenoxy)-7-methylquinoline-3-carbaldehyde) is a potential lead candidate for the development of a new antimalarial drug.

Keywords: Malaria; Mefloquine; Binding energy; Drug leads; Oral bioactivity score; Pharmacokinetics; Docking

1. Introduction

Malaria, a significant infectious disease characterized by acute febrile illness, continues to pose a global health concern. The World Health Organization estimates that the global

burden of malaria in the year 2020 ranged between 200 and 300 million cases, resulting in approximately 627,000 deaths[1]. Among the various species of *Plasmodium* that cause malaria, *Plasmodium falciparum* is the most formidable and widespread in Africa[2]. In the recent decades, drug-resistant strains of *P. falciparum* have emerged, leading to a worrisome situation where the effectiveness of currently available drugs has diminished. These persistent challenges have prompted the search for new drugs or the redesigning of existing chemical compounds, aiming to establish a sustainable global public health strategy.

An emerging approach to combat drug resistance in malaria involves exploring alternative biological components distinct from the traditional target sites. Plasmepsins, a type of aspartic proteinase present in malaria parasites, have emerged as promising targets for malaria treatment[3]. Histoaspartic protease (HAP) is one of the four plasmepsins found in the food vacuole of *P. falciparum*[4]. During the growth phase of the *Plasmodium* parasite, HAP is responsible for catalyzing the degradation of erythrocyte hemoglobin at specific peptide bonds, which serve as cleavage sites in the degradation pathway. This degradation process provides the parasite with essential amino acids for protein nutrient enrichment[5], whereas the other plasmepsins play different roles[6].

An effective strategy to inhibit the protease activity of the *Plasmodium* parasite is to target the active site of HAP, considering the presence of the aspartate residue (Asp215) and histidine residue (His32) in it. The high affinity of the aspartic protease inhibitor pepstatin-A for this active site makes it a potential candidate for blocking the

functionality of HAP and thereby inhibiting the protease of the *Plasmodium* parasite[7]. By disabling HAP's ability to degrade hemoglobin, the propagation of the parasite within host cells could be reduced while preserving the hemoglobin of infected erythrocytes.

Quinoline is a major component of these drugs. As an important organic compound found in certain natural compounds such as alkaloids and pharmacologically active substances, quinoline has been reported to exhibit inhibitory effects on *Plasmodium* proteases both *in vitro* and *in vivo*[8].

Figure 1 illustrates the presence of quinoline moieties (highlighted in red) in some current standard antimalarial drugs, whereas Figure 2 shows the presence of phenolic groups (red ring) at position 2 of quinoline derivatives, which are also found in various pharmacologically active compounds with antibacterial, anthelmintic, anticancer, antifungal, antihypertensive, anti-inflammatory, analgesic, and antiviral properties[9-12].

The drug-targeted design of quinoline derivatives as inhibitors of HAP is currently lacking substantial information. Therefore, our study aimed to assess the relative binding affinity of hypothetical quinoline derivatives with HAP of *P. falciparum* using *in silico* methods. We chose HAP of *P. falciparum* specifically because it possesses a unique, divergent vacuolar plasmepsin, which is distinct from the plasmepsin of any known *Plasmodium* species[13,14].

To study the relative binding affinity of hypothetical quinoline derivatives with HAP of *P. falciparum*, we synthesized 2-(2-benzoyl-4-methylphenoxy)quinoline-3-carbaldehyde (5 in Scheme 1; Figures S1–S3) and
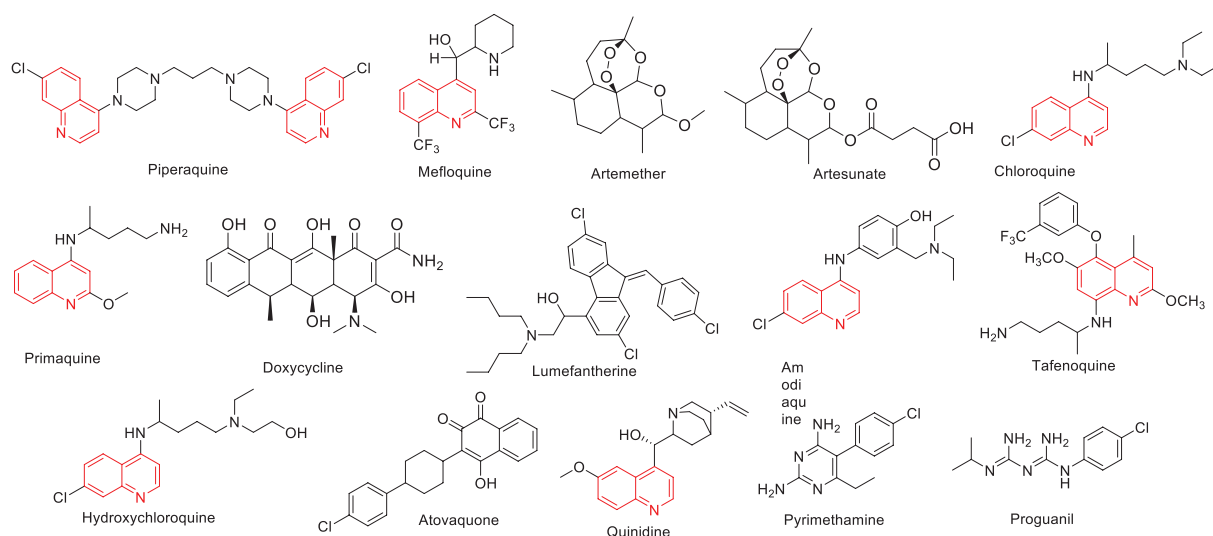
Figure 1. Common antimalarial drugs (mostly containing quinoline moieties).
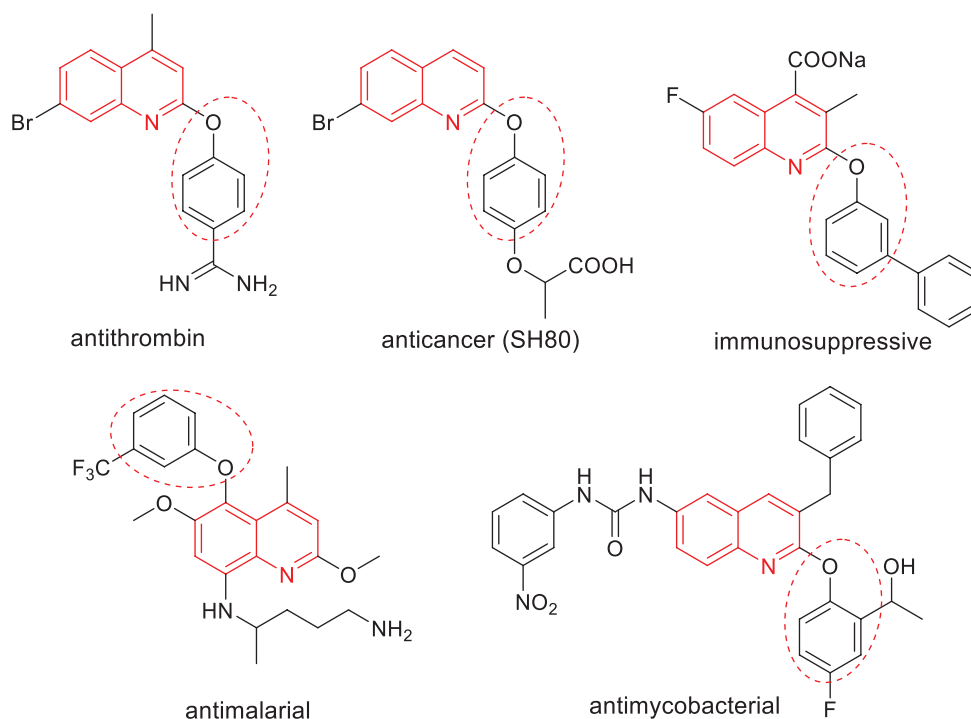
Figure 2. Properties of 2-phenoxyquinoline derivatives.
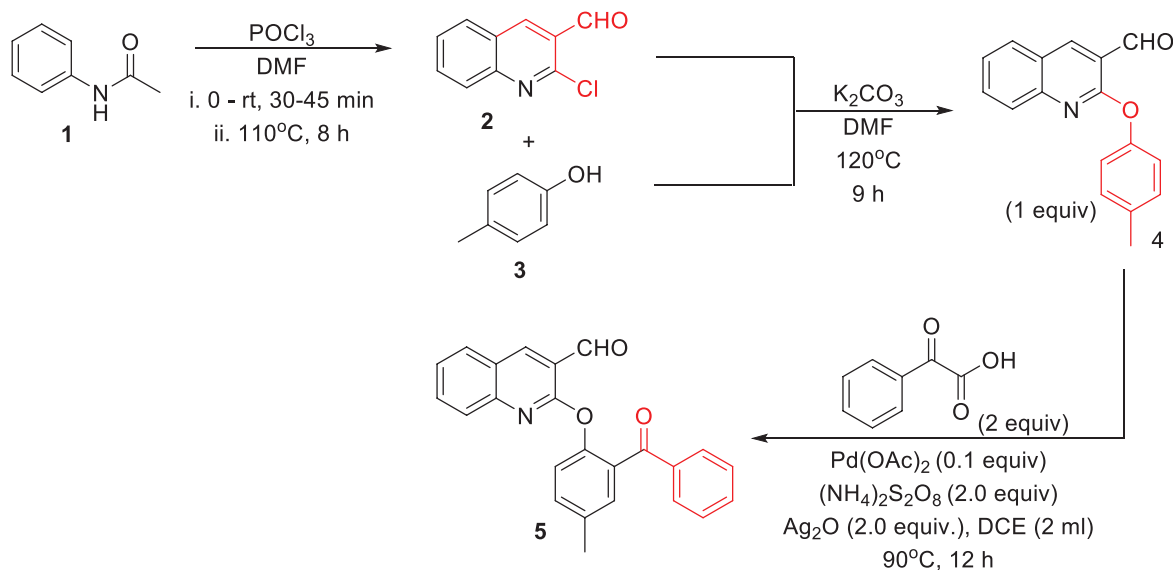
Scheme 1. Synthesis of 2-(2-benzoyl-4-methylphenoxy)quinoline-3-carbaldehyde (5).

evaluated its *in silico* toxicity, which was found to be mildly carcinogenic (Table 1). Subsequently, we designed 50 hypothetical derivative compounds (Figure 3) for *in silico* screening, aiming to identify lead candidates for antimalarial activity based on absorption, distribution, metabolism, excretion, and toxicity (ADMET) tests. Furthermore, we conducted investigations on their pharmacokinetics and bioactivity scores and performed molecular docking simulations into the binding pockets of HAP of *P. falciparum*. This drug-design protocol enabled us to gain insights into the binding interactions between the ligand compounds and the amino acid residues of the HAP enzyme's active sites, which represent a crucial aspect in the development of potential drug-like inhibitors.

Figure 3. Nine non-toxic hypothetical derivatives of compound 5.

2. Methodology

2.1. Synthesis of 2-(2-benzoyl-4-methylphenoxy) quinoline-3-carbaldehyde (5)

The synthesis of 2-(2-benzoyl-4-methylphenoxy)quinoline-3-carbaldehyde (5) involves three steps, which are described as follows:

2.1.1. Synthesis of 2-chloroquinoline-3-carbaldehyde (2)

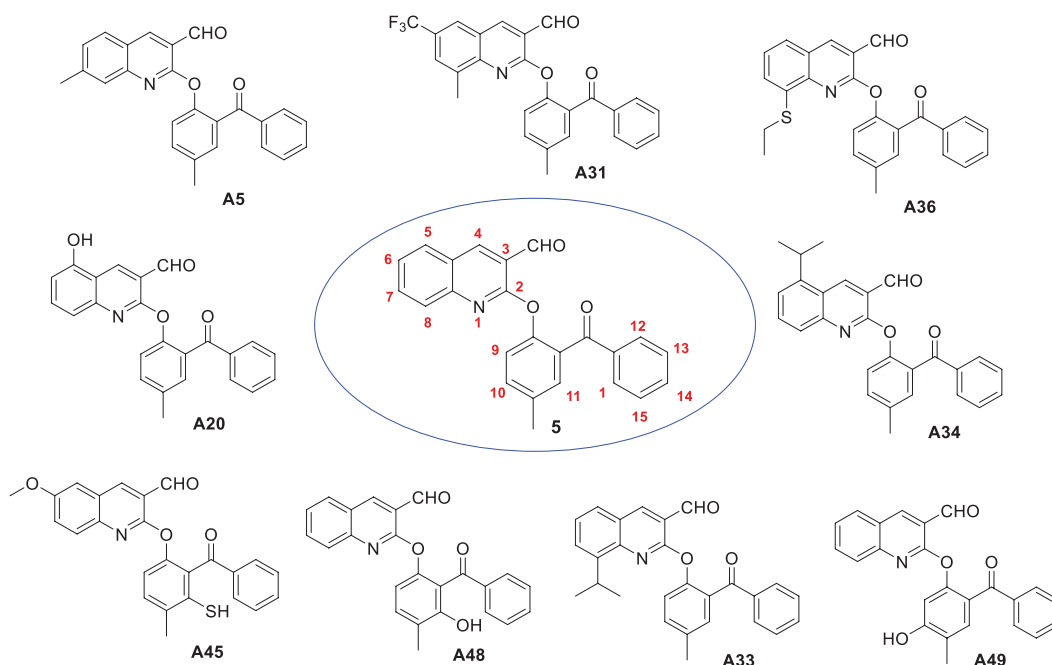Phosphorous oxychloride (POCl₃; 28 ml) was added dropwise to dimethylformamide (DMF) in a round-bottom flask while maintaining it an ice bath at 0°C. During this process, an orange color change was observed. The resulting mixture was then combined with acetanilide (10 g, 1 equivalent) dissolved in 30 ml of DMF. The temperature of the reaction was raised from 0°C to 80°C and maintained for 9 h. Thin-layer chromatography was used to monitor the progress of the reaction. After completion, the reaction mixture was allowed to cool and then slowly poured into an ice bath while stirring for 30 min. The resulting precipitate was washed with distilled water (50 ml × 5) to remove any residual acid. The precipitate was then filtered and left to air-dry for 48 h.

2.1.2. 2-(p-tolyloxy)quinoline-3-carbaldehyde (4)

Next, a mixture of *p*-cresol (1.70 ml, 10.44 mmol) and K₂CO₃ (4.33 g, 31.32 mmol) in 15 ml of DMF was prepared, and to this mixture, the precipitate obtained in the previous step, i.e., 2-chloroquinoline-3-carbaldehyde (2) (2.00 g,

10.44 mmol), was added. The reaction mixture was stirred at 90°C for 9 h. Upon completion, water (15 ml × 3) was added to the reaction mixture, and the resulting solid was filtered and recrystallized from ethyl acetate (10 ml). This yielded a white solid, 2-phenoxyquinoline-3-carbaldehyde (4), which served as the precursor for the benzoylation reaction.

2.1.3. Synthesis of 2-(2-benzoyl-4-methylphenoxy) quinoline-3-carbaldehyde (5)

A mixture of ammonium thiosulfate, (NH₄)₂S₂O₈ (0.24 g, 2.0 equivalents), and Ag₂O (a co-oxidant; 1.0 equivalent) was added to 2-phenoxychloroquinoline-3-carbaldehyde (4) (0.10 g, 0.38 mmol, 1.0 equivalent) in an oven-dried reaction tube, and Pd(OAc)₂ (0.008 g, 0.04 mmol, 0.1 equivalent) was used as a catalyst. The reaction mixture was flushed with nitrogen to remove air, and then dichloroethane (2 ml) was added before sealing the reaction vessel. The mixture was stirred at 100°C for 12 h with thin-layer chromatography monitoring. After completion, ethyl acetate (20 ml × 3) was used to extract the product. The organic layer was washed with water (15 ml × 3), dried with anhydrous sodium sulfate, filtered, and concentrated under vacuum. The resulting residue was purified through column chromatography on silica gel (60–120 mesh) using a hexane: ethyl acetate (1:19) solvent system, yielding compound 5 (2-phenoxyquinoline-3-carbaldehyde) in a 60% yield. The product's characterization was carried out using

A

B
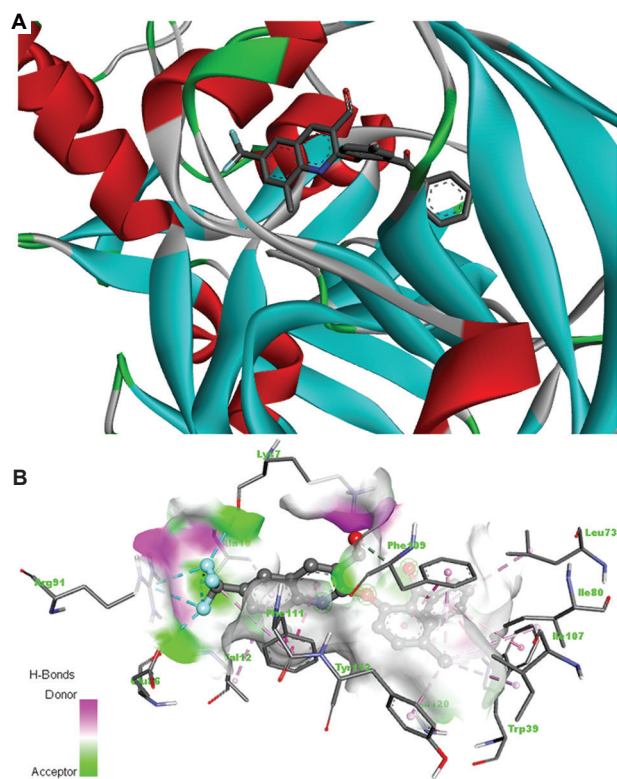
Figure 4A. (A and B) 3D interaction diagram and hydrogen bond donor and acceptor interaction of compound A31 with *Plasmodium falciparum* histoaspartic protease residues.

A

B

Figure 4B. (A and B) 2D diagram of the bond length and interacting residues of *Plasmodium falciparum* histoaspartic protease with compound A31.
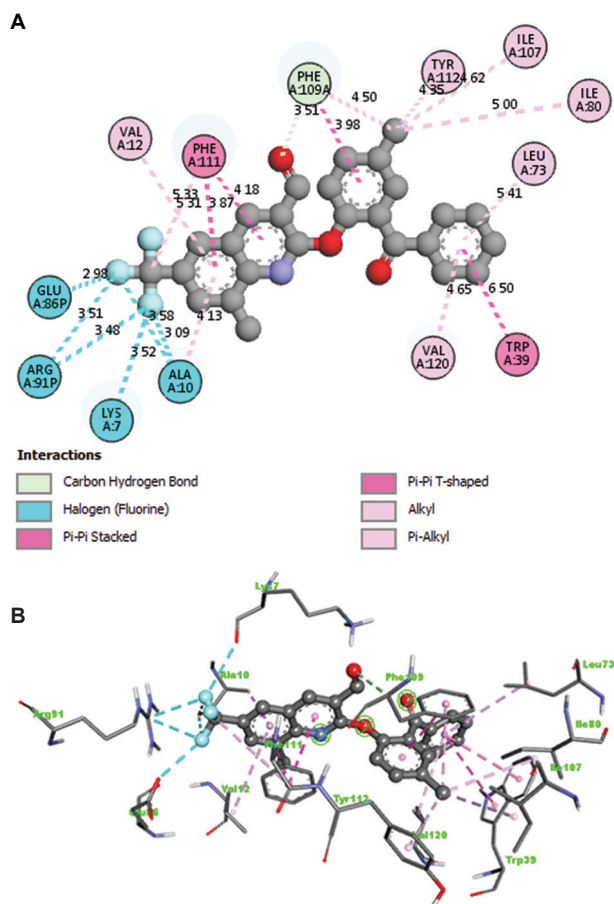
Fourier transform-infrared spectroscopy (FT-IR), proton nuclear magnetic resonance (^{1}H-NMR), and high-resolution mass spectrometry (HRMS) techniques.

2.1.4. Structural elucidation of compound 5

A white solid was obtained after a reaction time of 12 h with a yield of 60 %; m.pt: 119 – 121°C; IR (neat) *v* max (cm^{-1}) 3057, 2922, 2856, 2739, 1754, 1690, 1612, 1590, 1494, 1461, 1343, 1257, 1199, 1097, 760; ^{1}H-NMR (400 MHz, CDCl$_3$) δ 9.75 (s, 1H), 8.32 (s, 1H), 7.97 (d, *J* = 8.3 Hz, 1H), 7.82 (d, *J* = 8.2 Hz, 1H), 7.80 (t, *J* = 8.2 Hz, 1H), 7.74 (t, *J* = 7.5 Hz, 1H), 7.61 (d, *J* = 8.2 Hz, 1H), 7.51 (d, 1H), 7.39 (t, 1H), 7.19 (s, 1H), 6.86 (d, 1H), 6.84 (d, 1H), 2.41 (s, 3H). HRMS (ESI): Calc. for [(C$_{24}$H$_{17}$NO$_3$)] (M+H)$^+$ 368.1281, found 368.1283.

2.2. Toxicity prediction of compound 5

The synthesized compound 5 was subjected to toxicity testing by inputting its SMILES representation, which was drawn using ChemDraw 14.0 and saved as an.sdf file. The Protox II web server (https://tox-new.charite.de/protox_II/) was utilized for this purpose. The web server provided data on hepatoxicity, carcinogenicity,

immunotoxicity, mutagenicity, and cytotoxicity, which were then extracted[13].

2.3. Preparation of hypothetical compounds (A1–A50) and antimalarial reference drugs

A set of 50 hypothetical compounds were generated and visually represented using ChemDraw 14.0. These structures were saved in the.sdf format, and their corresponding SMILES notations were uploaded into the Protox II web server[15], as depicted in Figure 4. In addition, ten antimalarial drugs, namely, artesunate, doxycycline, tafenoquine, amodiaquine, artemether, lumefantrine, primaquine, piperaquine, mefloquine, and chloroquine, were obtained from PubChem[16] for comparative purposes. The structures of these drugs were downloaded and saved in the.sdf format, and their corresponding SMILES representations were also uploaded into the Protox II web server[16] to conduct virtual screening. This screening aimed to investigate their toxicity profiles and assess their compliance with all drug-likeness rules as outlined by Lipinski *et al.*[17]
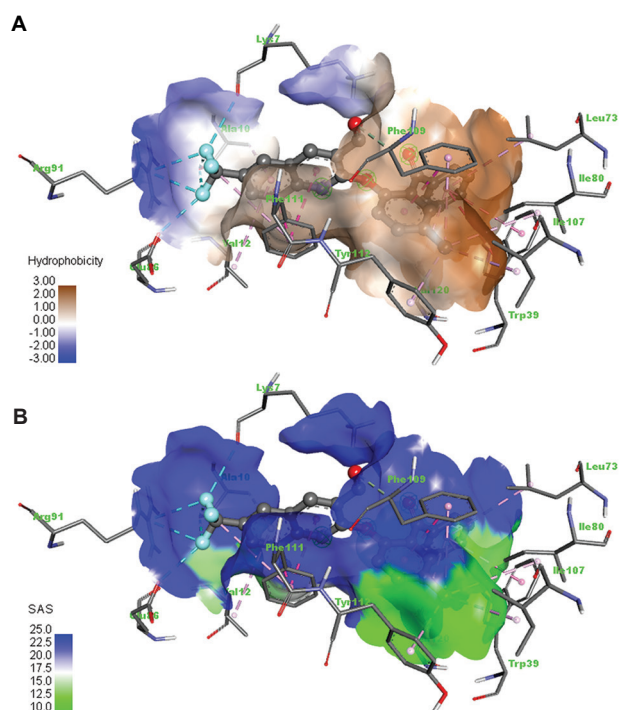
Figure 4C. (A and B) Hydrophobic/hydrophilic and solvent accessibility surface interaction of compound A31 with *Plasmodium falciparum* histoaspartic protease residues.

2.4. Selection of HAP protein receptor

The crystal structure of the HAP protein molecule, with a resolution of 2.10 Å, was acquired from the Protein Data Bank at rcsb.org[18]. The structure was obtained in the.pdb format and subsequently processed using BIOVIA Discovery Studio DS 2020 to eliminate any unwanted ligands and water molecules. In addition, polar hydrogen atoms were added to the structure as required.

2.5. *In silico* drug-likeness and ADME predictions

Compounds A1–A50 were subjected to drug-likeness analysis utilizing admetSAR2[19] to predict crucial adsorption, distribution, metabolism, and excretion (ADME) parameters for potential drug candidates[20]. The SMILES representations of these compounds were uploaded onto the web server, and the generated results were extracted and thoroughly analyzed.

2.6. Bioactivity score

To assess their suitability as drug candidates, compounds A1–A50 underwent drug-likeness analysis using admetSAR2[19]. This analysis aimed to predict vital parameters related to ADME for these compounds, with the goal of identifying potential candidates for further

drug development[20]. The SMILES representations of the compounds were submitted to the web server, and the resulting data were carefully extracted and comprehensively examined.

2.7. Molecular docking study

To evaluate the inhibitory potential of synthesized compound 5, as well as the selected hypothetical compounds, docking simulations were performed against HAP using the PyRx 0.8 AutoDock Vina Wizard. The macromolecules were converted to Autodock format, and a flexible ligand to rigid protein approach was employed. All possible binding sites on the target protein were explored during the docking process. The docking calculations were performed within a cubic grid of dimensions $90 \times 75 \times 60$ centered on the protein, encompassing the entire protein structure. This process lasted approximately 1 h. A grid spacing of 1.00 Å was utilized to generate the grid maps using the autogrid module of AutoDock Tools. Each ligand underwent nine independent runs to ensure accuracy.

Based on the identified potential binding sites, energetically favorable binding conformations were selected using AutodockVina[21]. The binding modes, along with their respective binding affinities and RSB (upper and lower) values, were obtained to guide the selection of the highest scoring binding conformation for each ligand. The binding mode with the best binding affinity was chosen. The ligand-protein complexes were analyzed using DS Visualizer. All software applications were executed on PC-based machines running the Microsoft Windows 10 operating system.

3. Results and discussion

3.1. Synthesis of 2-(2-benzoyl-4-methylphenoxy) quinoline-3-carbaldehyde (5) and preparation of hypothetical compounds (A1–A50) as ligands

Compound 5, which is 2-(2-benzoyl-4-methylphenoxy) quinoline-3-carbaldehyde, was synthesized through a series of steps starting from 2-phenoxyquinoline, derived from 2-chloroquinoline-3-carbaldehyde using the Vismeier-Haack formylation method (as discussed in Section 2.1 and depicted in Scheme 1). The characterization of compound 5 involved the use of FT-IR, HRMS, and ¹H-NMR spectroscopy (Figures S4–S9). In each step of the synthesis, newly added sections of the molecule were highlighted in red.

Initial docking studies revealed that compound 5 (2-(2-benzoyl-4-methylphenoxy)quinoline-3-carbaldehyde) displayed noteworthy bioactivity. However, it was also found to have a mild carcinogenic effect, as indicated in
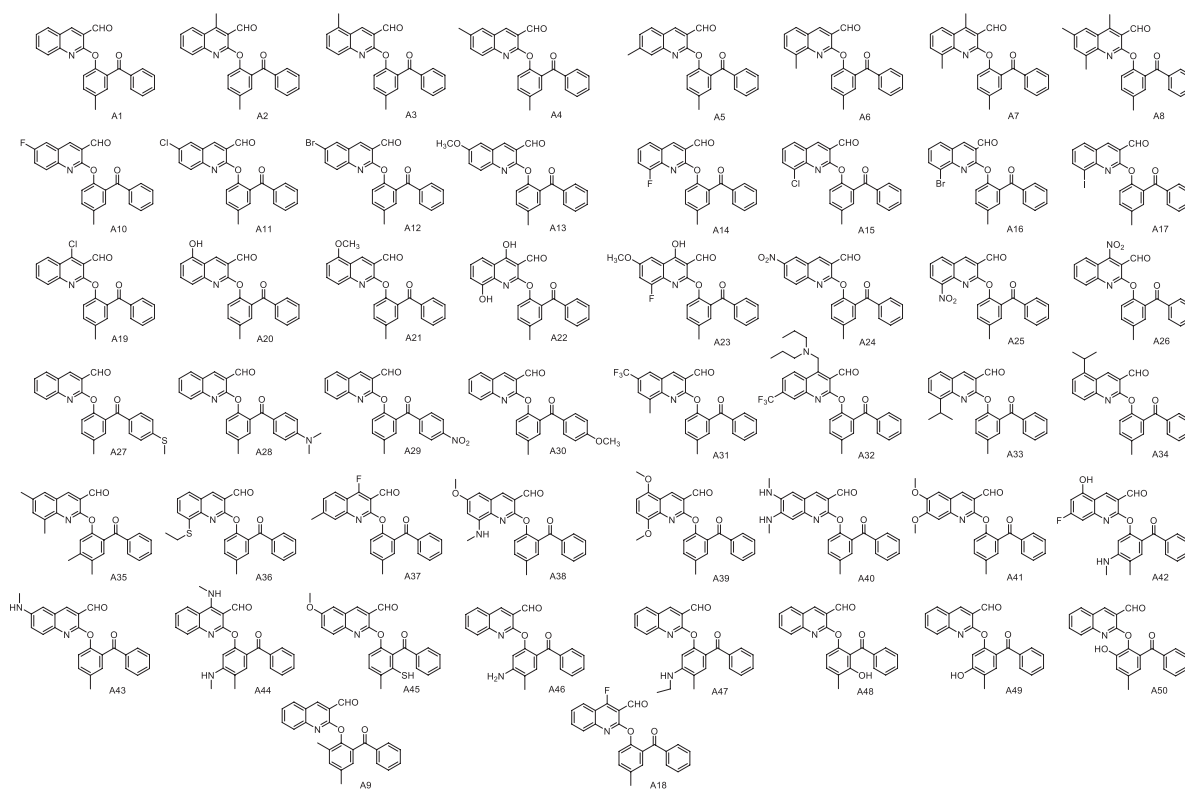
Figure 5. Hypothetical compounds A1–A50 obtained from structural modifications of compound 5.

Table 1. Toxicity prediction and probability values of lead compounds using Protox II webserver

Target	Compound 5	A5	A31	A36	A20
Hepatotoxicity	Inactive (0.56)	Inactive (0.97)	Inactive (0.50)	Inactive (0.52)	Inactive (0.54)
Carcinogenicity	Active (0.54)	Inactive (0.57)	Inactive (0.52)	Inactive (0.52)	Inactive (0.54)
Immunotoxicity	Inactive (0.83)	Inactive (0.99)	Inactive (0.82)	Inactive (0.71)	Inactive (0.67)
Mutagenicity	Inactive (0.55)	Inactive (0.85)	Inactive (0.56)	Inactive (0.56)	Inactive (0.60)
Cytotoxicity	Inactive (0.75)	Inactive (0.78)	Inactive (0.74)	Inactive (0.75)	Inactive (0.75)

Table 2. Toxicity prediction and probability values of lead compounds using Protox II webserver

Target	A33	A34	A45	A48	A49
Hepatotoxicity	Inactive (0.60)	Inactive (0.60)	Inactive (0.52)	Inactive (0.54)	Inactive (0.54)
Carcinogenicity	Inactive (0.56)	Inactive (0.56)	Inactive (0.51)	Inactive (0.41)	Inactive (0.54)
Immunotoxicity	Inactive (0.65)	Inactive (0.62)	Inactive (0.67)	Inactive (0.69)	Inactive (0.60)
Mutagenicity	Inactive (0.53)	Inactive (0.53)	Inactive (0.52)	Inactive (0.60)	Inactive (0.60)
Cytotoxicity	Inactive (0.71)	Inactive (0.71)	Inactive (0.76)	Inactive (0.75)	Inactive (0.75)

Table 1. Therefore, the rationale behind the research was to propose structural modifications by introducing various substituents at specific positions of the quinoline, tolyoxy, and benzoyl components of compound 5. These substituents included methyl, halogens, thiol, amino, methoxy, nitro, hydroxy, and isopropyl groups at positions 4, 5, 6, 7, and 8 of the quinoline moiety. For the tolyloxy scaffold, methyl, amino, thiol, and hydroxy groups were considered at the ortho and meta positions. Furthermore, for the *para* positions of the benzoyl scaffold, thiol, amino, nitro, and methoxy substituents were taken into account (Figure 5).

3.2. Toxicity results of compound (5), hypothetical compounds (A1–A50), and ten antimalarial reference drugs

A total of 50 hypothetical compounds (A1–A50) depicted in Figure 5, along with ten reference drugs (artesunate, doxycycline, tafenoquine, amodiaquine, arthemeter, lumefantrine, primaquine, piperaquine, mefloquine, and chloroquine), were subjected to virtual investigations to evaluate their toxicity profiles. The specific toxicity parameters examined included hepatoxicity, carcinogenicity, immunogenicity, mutagenicity, and cytotoxicity, as outlined in Table 1.

Notably, compound 5 and forty-one of the hypothetical derivatives exhibited failures in one or more of these tests, suggesting potential toxic and carcinogenic activities[22]. However, nine lead compounds (A5, A20, A31, A33, A34, A36, A45, A48, and A49) shown in Figure 3 demonstrated full compliance with the evaluated toxicity parameters (Tables 1 and 2).

Notably, the toxicity results for the reference drugs, as shown in Tables 3 and 4, revealed that only mefloquine demonstrated compliance with the evaluated parameters. In contrast, the other reference drugs exhibited one or more violations when compared to the nine lead compounds.

Table 3. Toxicity prediction of standard drugs against *P. falciparum* using Protox II webserver

Target	Mefloquine	Piperaquine	Artesunate	Doxycycline	Tafenoquine
Hepatotoxicity	Inactive (0.75)	Inactive (0.78)	Inactive (0.76)	Active (0.54)	Inactive (0.78)
Carcinogenicity	Active (0.76)	Inactive (0.71)	Inactive (0.65)	Inactive (0.77)	Inactive (0.63)
Immunotoxicity	Inactive (0.84)	Active (0.93)	Active (0.87)	Active (0.99)	Active (0.99)
Mutagenicity	Inactive (0.68)	Active (0.50)	Inactive (0.63)	Inactive (0.95)	Active (0.54)
Cytotoxicity	Inactive (0.74)	Inactive (0.82)	Inactive (0.87)	Inactive (0.90)	Inactive (0.63)

Table 4. Toxicity prediction of standard drugs against *P. falciparum* using Protox II webserver

Target	Amodiaquine	Artemether	Lumefantrine	Primaquine	Chloroquine
Hepatotoxicity	Inactive (0.61)	Inactive (0.77)	Inactive (0.70)	Inactive (0.84)	Inactive (0.90)
Carcinogenicity	Active (0.61)	Inactive (0.66)	Inactive (0.61)	Inactive (0.59)	Inactive (0.66)
Immunotoxicity	Active (0.99)	Active (0.92)	Active (0.99)	Active (0.99)	Active (0.69)
Mutagenicity	Inactive (0.75)	Inactive (0.60)	Inactive (0.60)	Active (0.79)	Active (0.94)
Cytotoxicity	Inactive (0.53)	Inactive (0.94)	Inactive (0.67)	Inactive (0.61)	Inactive (0.93)

Table 5. Physicochemical properties and drug-likeness of lead compounds using SwissADME webserver

Physico*	5	A5	A31	A36	A20	A33	A34	A45	A48	A49	Mefloq
MW	367.40	381.42	449.42	427.51	383.40	409.48	409.48	429.49	383.40	383.40	378.31
#rot_b	5	5	6	7	5	6	6	6	5	5	4
#HA	4	4	7	4	5	4	4	5	5	5	9
#HD	0	0	0	0	1	0	0	0	1	1	2
TPSA	56.26	56.26	56.26	81.56	76.49	56.26	56.26	104.29	76.49	76.49	45.15
natoms	28	29	33	31	29	31	31	31	29	29	26
nviol	1	1	1	1	1	1	1	1	1	1	2
log Kp	−4.83	−4.66	−4.45	−4.58	−5.18	−4.29	−4.29	−5.13	−4.79	−5.18	−6.04
Bioav	0.55	0.55	0.55	0.55	0.55	0.55	0.55	0.55	0.55	0.55	0.55
GI	High	High	Low	Low	High	High	High	Low	High	High	High
BBB	Yes	No	No	No	No	No	No	No	No	No	No
Pgp	No	No	Yes	Yes	No	Yes	Yes	No	No	No	Yes

Abbreviations: TPSA: Total polar surface area; natoms: Number of atoms in the molecule; MW: Molecular weight; #HA: Number of hydrogen bond acceptors; #HD: Number of hydrogen bond donors; nviol: Number of violations; #rot_b: Number of rotatable bonds; bioav: Bioavailability; GI: Gastrointestinal absorption; BBB: Blood–brain barrier; Pgp: Permeability glycoprotein substrate; Mefloq: Mefloquine.

Table 6. Drug violations and cytochrome inhibition ability of compound 5 and the leads using SwissADME webserver

Derivative	Lipinski	Ghose	Veber	Egan	Muegge	CYP2C19	CYP2D6
5	0	0	0	0	1	Yes	No
A5	0	1	0	0	1	Yes	No
A31	1	1	0	1	1	Yes	No
A36	0	1	0	1	1	Yes	No
A20	0	0	0	0	0	Yes	No
A33	0	1	0	1	1	Yes	No
A34	0	1	0	1	1	Yes	No
A45	0	1	0	0	1	Yes	No
A48	0	0	0	0	1	Yes	No
A49	0	0	0	0	0	Yes	No

Based on this finding, mefloquine was chosen for further virtual studies alongside the selected lead compounds.

3.3. *In silico* drug-likeness and ADME predictions

The results presented in Table 5 indicate that the lead compounds exhibit characteristics in compliance with the Rule of Five (RO5). These compounds have a suitable number of hydrogen bond donors (0–1 for nitrogen-hydrogen and oxygen-hydrogen bonds) and hydrogen bond acceptors (4–7 for nitrogen or oxygen atoms), which fall within the recommended ranges (<5 and <10, respectively). Their molecular weights range from 367.40 to 449.40 g/mol, aligning with the guideline of 150 to 500 g/mol. The observed topological polar surface area (TPSA) values range from 56.26 to 104 Å2, which also conform to the acceptable range of 20 to 130 Å2. In addition, the number of rotatable bonds in these compounds does not exceed 9.

According to a previous reported by Daina *et al.*[23], the negative log Kp values (−5.13 to −5.18) suggest that compounds A20, A45, and A49 are predicted to have lower permeability through human skin compared to the other compounds. On the contrary, compounds A31, A36, and A45 exhibit reduced gastrointestinal absorption rates. These characteristics can be attributed to specific structural features, such as the presence of a trifluoromethyl group at position 6 in compound A31, a thiol group at position 8 in compound A36, and a combination of a methoxy group at position 6 and a thiol group at position 3 in the methylphenoxyl ring. Notably, compound 5 displays permeability through the blood–brain barrier, unlike the other lead compounds. Furthermore, compounds A31, A33, A34, and A36 are identified as substrates for P-glycoprotein (P-gp) based on the studies conducted by Daina *et al.* Klopman *et al.*[23,24].

Out of the nine lead compounds, six, including compound 5, exhibited high gastrointestinal absorption

Table 7. Binding energies of pure derivatives and reference drugs

Ligand	Binding affinity
A31_uff_E=300.34	−11.3
A5_uff_E=278.30	−11.2
A1/5_uff_E=277.56	−10.9
A20_uff_E=282.50	−10.8
A33_uff_E=300.83	−10.5
A49_uff_E=284.88	−10.5
A48_uff_E=343.12	−9.9
A36_uff_E=283.54	−9.8
A45_uff_E=414.27	−9.8
Mefloquine	−9.6
Piperaquine	−9
A34_uff_E=340.75	−8.7
Artesunate	−8.5
Doxycycline	−8.5
Tafenoquine	−8.5
Amodiaquine	−8.4
Artemether	−8.3
Lumefantrine	−7.3
Primaquine	−6.9
Chloroquine	−6

rates, except for A31, A36, and A45. Moreover, unlike the other lead compounds, compound 5 has the ability to penetrate the blood–brain barrier, as indicated in Table 5. All nine lead compounds demonstrate good oral bioavailability, with a value of 0.55, with only one permissible violation according to Lipinski *et al.*[25] The inhibition of cytochrome P450 (CYP) isoenzymes is recognized as a major factor contributing to pharmacokinetics-related drug–drug interactions[26]. Such

interactions can lead to toxic or adverse effects due to decreased drug clearance or the accumulation of drugs or their metabolites. Table 6 reveals that the lead compounds act as inhibitors of CYP2C19 while serving as substrates for CYP2D6. These cytochromes play crucial roles in the metabolism and elimination of approximately 25% of
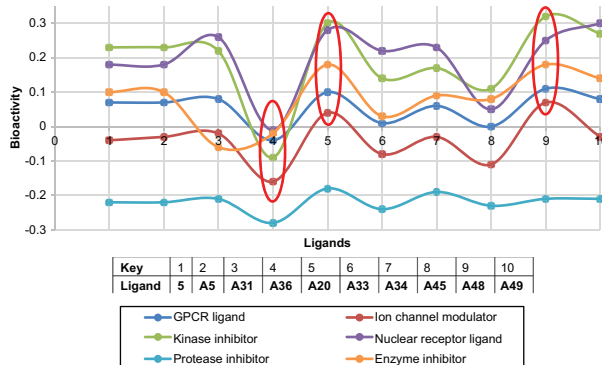
clinically utilized drugs, involving the addition or removal of specific functional groups through hydroxylation, demethylation, and dealkylation processes[27].

3.4. Bioactivity score

The potential candidacy of drug leads can be assessed by evaluating their bioactivity scores. In Figure 6, it can be observed that all the lead compounds generally exhibit high or moderate bioactivity across various parameters. Specifically, compounds A20 and A48 display high activity in five out of the six parameters, with bioactivity scores ranging from 0.00 to 0.33. Compounds A5 and A31 demonstrate high bioactivity as kinase inhibitors (with scores of 0.23 and 0.22, respectively), which suggests their potential in inhibiting cancer cells[28]. They also exhibit high bioactivity as nuclear receptor ligands (with scores of 0.18

Figure 6. Bioactivity score of pure derivatives in compliance with the Pearson's correlation coefficient.
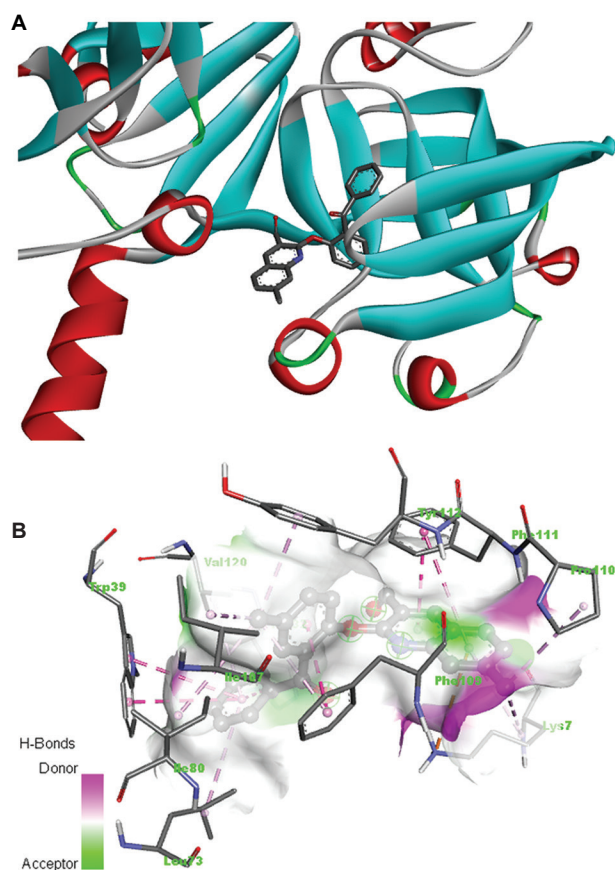

Figure 7A. (A and B) 3D interaction diagram and hydrogen bond donor and acceptor interaction of compound A5 with *Plasmodium falciparum* histoaspartic protease residues.
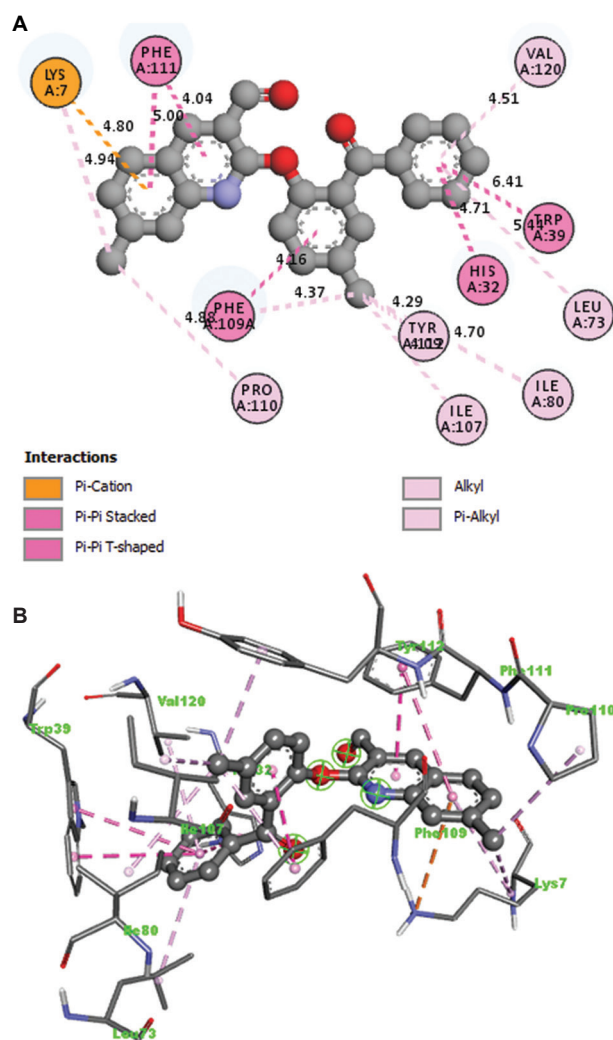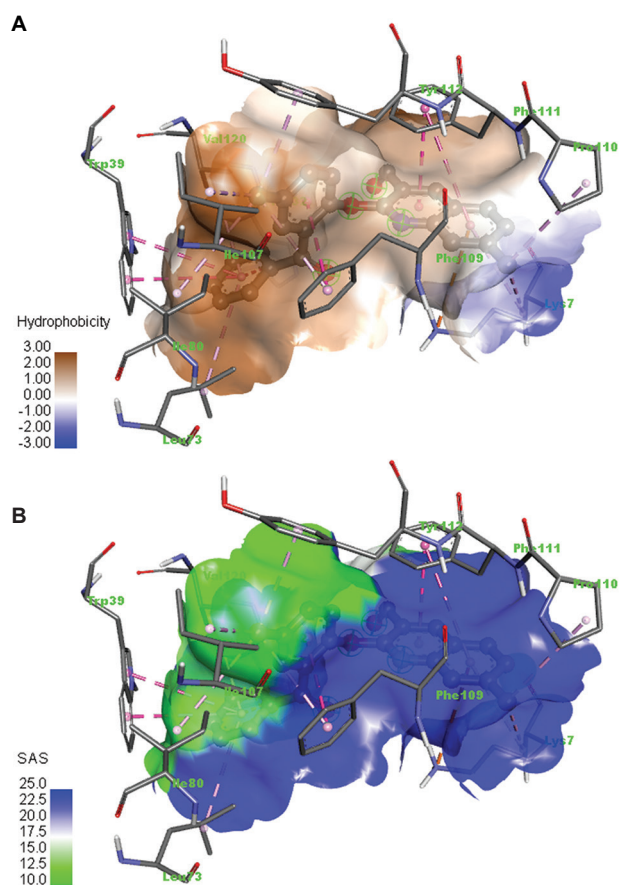

Figure 7B. (A and B) 2D diagram of the bond length and interacting residues of *Plasmodium falciparum* histoaspartic protease with compound A5.
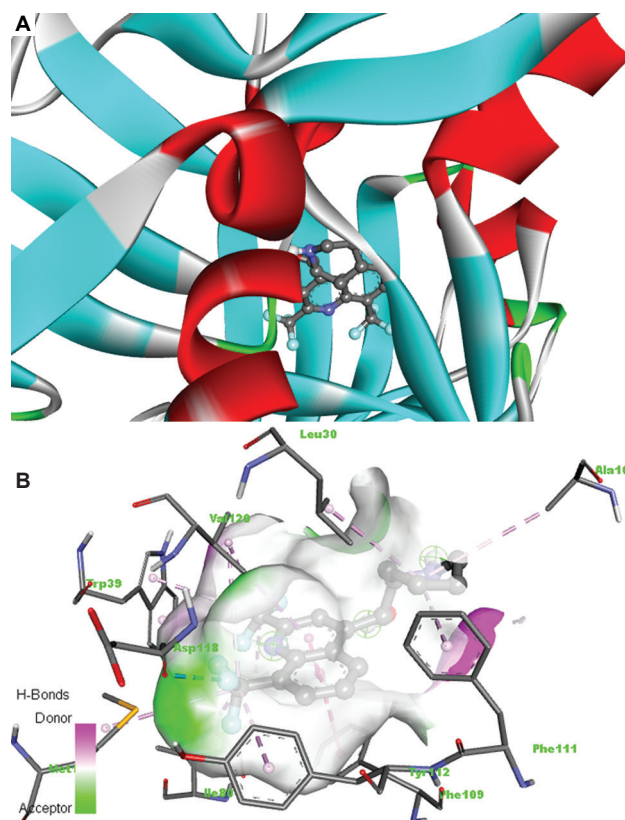
A

B

Figure 7C. (A and B) Hydrophobic/hydrophilic and solvent accessibility surface interaction of compound A5 with *Plasmodium falciparum* histoaspartic protease residues.

A

B

Figure 8A. (A and B) 3D interaction diagram and hydrogen bond donor and acceptor interaction of mefloquine with *Plasmodium falciparum* histoaspartic protease residues.

and 0.26, respectively), indicating their ability to interact with hydrophobic molecules such as fatty acids, cholesterol, and lipophilic hormones[29]. Furthermore, compounds A5 and A31 demonstrate bioactivity as glycoprotein receptors GPCR (with scores of 0.07 and 0.08, respectively), which regulate metabolic enzymes and promoter proteins, among other functions[30]. Compound A5 is also an enzyme inhibitor (with a score of 0.1), indicating its capability to bind to additional sites on the enzyme[31]. Among the lead compounds, A36 exhibits the lowest bioactivity score.

In terms of protease inhibition, all the lead compounds display moderate activity (with scores ranging from −0.18 to −0.28), suggesting their potential to impede the maturation of new HIV cells[32]. Only compounds A20 and A48 exhibit high activity as ion channel modulators, with scores of 0.04 and 0.07, respectively, surpassing the threshold of 0.00[33].

3.5. Molecular docking study

The findings from the docking simulations of ligands and reference drugs against HAP are summarized in Table 7.

The binding energies for compound A31 (−11.3 kcal/mol) and compound A5 (−11.2 kcal/mol) are higher than that of compound 5 (−10.9 kcal/mol). Furthermore, the following six lead compounds exhibit binding energies ranging from −10.8 to −9.8 kcal/mol, all of which are higher than those of the ten reference drugs examined. Among the reference drugs, mefloquine performs the best with a binding energy of −9.6 kcal/mol, whereas chloroquine displays the lowest binding energy of −6.0 kcal/mol.

In Figures 4A, 7A, and 8A, the interaction between hydrogen acceptors and donors is depicted. In this representation, the donor group (indicated by a pink region, typically a hydrogen atom) from the ligand engages with the hydrogen bond acceptor site (depicted in green) on the surface of the enzyme. This electrostatic attraction between the partially positively charged hydrogen atom and the lone pair of electrons on the acceptor atom contributes to the stability of the molecular complexes formed, as illustrated in Figures 4, 7, and 8. Such interactions play a vital role in various biological and chemical processes, including protein-ligand binding, DNA base pairing, and solvation phenomena in the
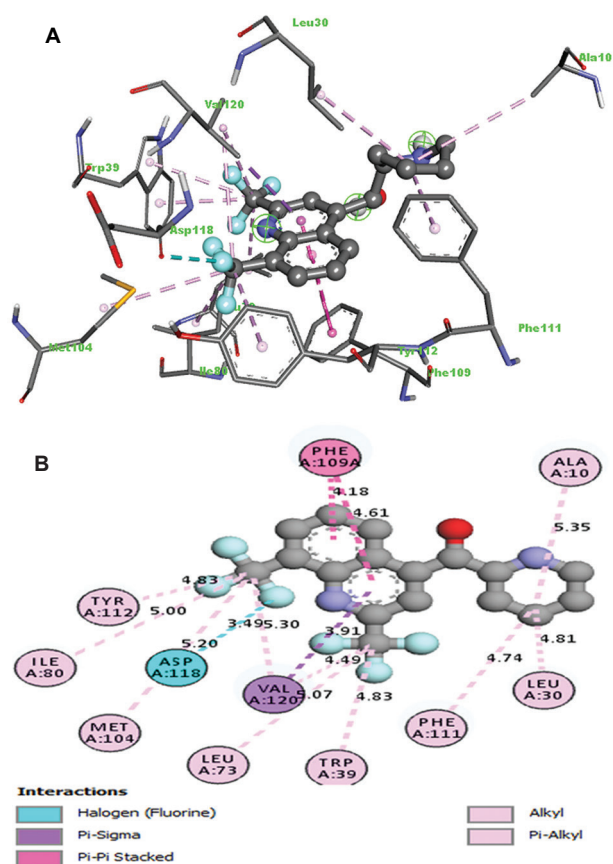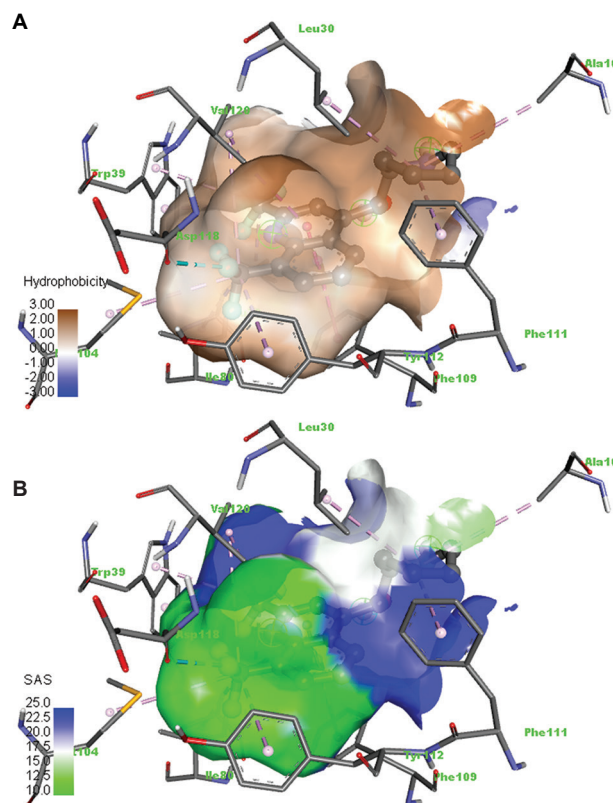
Figure 8B. (A and B) 2D diagram of the bond length and interacting residues of *Plasmodium falciparum* histoaspartic protease with mefloquine.

Figure 8C. (A and B) Hydrophobic/hydrophilic and solvent accessibility surface interaction of mefloquine with *Plasmodium falciparum* histoaspartic protease residues.

context of the *P. falciparum* HAP (PDB ID: 3QVC) and the lead compounds.

In the 2D view shown in Figure 4B, we observed hydrogen-binding interactions between the carbaldehyde oxygen atom of the quinoline core and Phe109, with a bond length of 3.51 Å. In addition, the strong fluorine bonds formed by the trifluoromethyl groups at position 7 with Glu86, Arg91, Lys7, and Ala10 (bond lengths ranging from 2.98 to 3.58 Å) likely contribute to the potent inhibitory interactions of 2-(2-benzoyl-4-methylphenoxy)-8-methyl-6-(trifluoromethyl) quinoline-3-carbaldehyde (A31) with *P. falciparum* (HAP). Other types of bonds observed in the interaction, as depicted in Figure 4B, include alkyl, π-π alkyl, π-π stacked, and π alkyl interactions at various bond lengths with residues of the protein.

Hydrophobic interactions (Figure 4C) are highly crucial for the folding of proteins, especially in keeping the protein stable and biologically active through decrease in surface area, thereby reducing the undesirable interactions with water[34]. Herein, compound A31 exhibits hydrophobic interactions with the *P. falciparum* HAP amino acid residues, especially

the 2-benzoyl-4-methylphenoxy side of the molecule interacting with Leu_{73}, Ile_{80}, Tyr_{112}, Phe_{111}, Trp_{39}, and Ile_{107}.

The interaction of the trifluoromethyl side of the quinoline molecule with Glu86, Arg91, Lys7, and Ala10 exhibits a distinct hydrophilic nature, attributed to the electronegative character of the fluorine atom. Solvent accessibility plays a significant role in protein folding and stability[35]. In Figure 4C, the solvent accessibility surface is represented by the blue region, indicating a large surface area. This suggests that compound A31 has a favorable interaction with the binding pocket of the HAP protein, potentially leading to enhanced binding and stability.

Similarly, the 3D structure of compound A5 is shown in Figure 7A with binding energy of −11.2 kcal/mol. The absence of hydrogen bond does not reduce its efficacy as HAP inhibitor due to other interactions such as π-cation (π electrons of the quinoline core and the amino hydrogen of the side chain of Lys_7), alkyl and π-alkyl (ligand and amino acid residues such as Val120, Leu73, Tyr410, Leu73, Ile80, Ile107, and Pro110), and π-π stacked and π-π T-shaped (compound A5 and Phe111, Phe109, His32, and Trp39) all contributed to its high binding energy (Figure 7B).

Figure 7C reveals that compound A5 exhibits notable hydrophobic interactions with all observed binding residues, except for Lys7. This observation suggests that compound A5 may possess favorable water–lipid interface transport properties, facilitating its movement across the cell membrane of the Pf HAP protein. In addition, the quinoline core of compound A5 demonstrates improved solvent accessibility, indicating a more open conformation. This conformation may promote easier interaction with the reactive sites of the target residues, as suggested by Gromiha and Ahmad[36].

The binding interactions between the best reference drug, mefloquine, and the residues of *P. falciparum* HAP (Figures 8A and 8B) indicate that the trifluoro groups attached to position 6 in compound A31 and position 8 in mefloquine play a role in their enhanced activity. However, unlike compound A31, mefloquine does not exhibit any hydrogen-bonding interactions, which could potentially contribute to its lower binding energy.

Similarly, the solvent accessibility surface interaction of compound A31 is greater than that of mefloquine, as indicated in Figure 8C, indicating a more favorable interaction within the binding pocket of the HAP protein.

4. Conclusion

In this study, we conducted toxicity profile tests to evaluate the synthesized compound 5 and fifty hypothetical compounds A1–A50 for their drug-likeness. The aim was to identify lead drug candidates that can overcome resistance to current standard reference antimalarial drugs. Among the hypothetical compounds, nine showed no toxicity to human cells.

Compounds A5 and A31 exhibited high bioactivity as kinase inhibitors, nuclear receptor ligands, and glycoprotein receptors GPCR. In addition, compound A5 acted as an enzyme inhibitor, capable of binding to other available sites on the HAP enzyme. It is hypothesized that the interaction of ligands at the active site of HAP, specifically the aspartate (Asp215) and histidine (His32) residues, can be treated as therapeutic targets, due to their importance for parasite growth and virulence, for developing effective inhibitors.

Interestingly, compound A31, with a binding energy of −11.3 kcal/mol, did not show any evidence of interaction with Asp215 or His32. However, compound A5, with a binding energy of −11.2 kcal/mol, exhibited π-π stacking interactions with His32. The best-performing reference drug, mefloquine, also did not show any interaction with Asp215 or His32.

Furthermore, compound A5 displayed significant hydrophobic interactions with all observed binding residues,

except Lys7. This suggests that it has good water–lipid interface transport properties within the cell membrane of the Pf HAP protein. In addition, the quinoline core of compound A5 had better solvent accessibility, indicating a more open conformation that facilitates binding with reactive sites on the target residues. Based on our study findings, compound A5 shows promise as a potential candidate for developing drugs against antimalarial diseases.

Acknowledgments

Funding

Conflict of interest

The authors declare they have no competing interests.

Author contributions

Conceptualization: Luqman A. Adams, Oluwole B. Familoni
Formal analysis: Oluwafemi S. Aina, Luqman A. Adams
Investigation: Oluwafemi S. Aina, Adebayo J. Bello
Methodology: Oluwafemi S. Aina, Adebayo J. Bello
Writing – original draft: Oluwafemi S. Aina, Luqman A. Adams
Writing – review & editing: Luqman A. Adams, Oluwole B. Familoni

Ethics approval and consent to participate

Not applicable.

Consent for publication

Not applicable.

Availability of data

Not applicable.

Further disclosure

The paper has been uploaded to or deposited in a preprint server (Research Square): https://doi.org/10.21203/rs.3.rs-2748975/v1

References

1.   World Health Organization, 2022, WHO Guidelines for Malaria. WHO/UCN/GMP/2022.01 Rev. 2. Geneva: World Health Organization.

2. Jensen AR, Adams Y, Hviid L, 2020, Cerebral *Plasmodium falciparum* malaria: The role of PfEMP1 in its pathogenesis and immunity, and PfEMP1-based vaccines to prevent it. *Immunol. Rev.*, 293: 230–252.

https://doi.org/10.1111/imr.12807

3. Karthik L, Kumar G, Keswani T, *et al.*, 2014, Protease inhibitors from marine actinobacteria as a potential source for antimalarial compound. *PLoS One*, 9: e90972.

4. Francis SE, Banerjee R, Goldberg DE, 1997, Biosynthesis and maturation of the malaria aspartic hemoglobinases plasmepsins I and II. *J Biol Chem*, 272: 14961–14968.

https://doi.org/10.1074/jbc.272.23.14961

5. Nasamu AS, Polino AJ, Istvan ES, 2020, Malaria parasite plasmepsins: More than just plain old degradative pepsins. *J Biol Chem*, 295: 8425–8441.

https://doi.org/10.1074/jbc.REV120.009309

6. Boddey JA, Hodder AN, Günther S, *et al.*, 2010, An aspartyl protease directs malaria effector proteins to the host cell. *Nature*, 463: 627–631.

https://doi.org/10.1038/nature08728

7. Roy KK, 2017, Targeting the active sites of malarial proteases for antimalarial drug discovery: Approaches, progress and challenges. *Int J Antimicrob Agents*, 50: 287–302.

https://doi.org/10.1016/j.ijantimicag.2017.04.006

8. Zhou W, Wang H, Yang Y, *et al.*, 2020, Chloroquine against malaria, cancers and viral diseases. *Drug Discov Today*, 25: 2012–2022.

https://doi.org/10.1016/j.drudis.2020.09.010

9. Hong SH, Ismail IA, Kang SM, *et al.*, 2016, Cinnamaldehydes in cancer chemotherapy. *Phytother Res*, 30: 754–767.

https://doi.org/10.1002/ptr.5592

10. Nair A, Amalraj A, Jacob J, *et al.*, 2019, Non-curcuminoids from turmeric and their potential in cancer therapy and anticancer drug delivery formulations. *Biomolecules*, 9: 13.

https://doi.org/10.3390/biom9010013

11. Ma HS, Wang EL, Xu WF, *et al.*, 2018, Overexpression of DNA (cytosine-5)-methyltransferase 1 (DNMT1) and DNA (cytosine-5)-methyltransferase 3A (DNMT3A) is associated with aggressive behavior and hypermethylation of tumor suppressor genes in human pituitary adenomas. *Med Sci Monit*, 24: 4841–4850.

https://doi.org/10.12659/MSM.910608

12. Schneidman-Duhovny D, Inbar Y, Nussinov R, *et al.*, 2005, Geometry-based flexible and symmetric protein docking. *Proteins*, 60: 224–231.

https://doi.org/10.1002/prot.20562

13. Banerjee R, Liu J, Beatty W, *et al.*, 2002, Four plasmepsins are active in the *Plasmodium falciparum* food vacuole, including a protease with an active-site histidine. *Proc Natl Acad Sci*, 99: 990–995.

https://doi.org/10.1073/pnas.022630099

14. Bhaumik P, Gustchina A, Wlodawer A, 2012, Structural studies of vacuolar plasmepsins. *Biochim Biophys Acta*, 1824: 207–223.

https://doi.org/10.1016/j.bbapap.2011.04.008

15. Available from: https://tox-new.charite.de [Last accessed on 2023 May 31].

16. Available from: https://pubchem.ncbi.nlm.nih.gov [Last accessed on 2023 May 25].

17. Lipinski B, Herzog H, Kops ER, *et al.*, 1997 Expectation maximization reconstruction of positron emission tomography images using anatomical magnetic resonance information. *IEEE Trans Med Imaging*, 16: 129–136.

https://doi.org/10.1109/42.563658

18. Available from: https://www.rcsb.org/ [Last accessed on 2023 Apr 20].

19. Available from: https://lmmd.ecust.edu.cn/admetsar2 [Last accessed on 2023 Mar 15].

20. Yang H, Sun L, Li W, *et al.*, 2018, *In silico* prediction of chemical toxicity for drug design using machine learning methods and structural alerts. *Front Chem*, 6: 30.

https://doi.org/10.3389/fchem.2018.00030

21. Trott O, Olson AJ, 2010, AutoDock Vina: Improving the speed and accuracy of docking with a new scoring function, efficient optimization, and multithreading. *J Comput Chem*, 31: 455.

https://doi.org/10.1002/jcc.21334

22. Jacobs AC, Hatfield KP, 2013. History of chronic toxicity and animal carcinogenicity studies for pharmaceuticals. *Vet Pathol*, 50: 324-333.

https://doi.org/10.1177/0300985812450727

23. Daina A, Olivier M, Vincent Z, 2017, SwissADME: A free web tool to evaluate pharmacokinetics, drug-likeness and medicinal chemistry friendliness of small molecules. *Sci Rep*, 7: 42717.

https://doi.org/10.1038/srep42717

24. Klopman G, Stefan LR, Saiakhov RD, 2002, ADME evaluation: 2. A computer model for the prediction of intestinal absorption in humans. *Eur J Pharm Sci*, 17: 253–263.

https://doi.org/10.1016/s0928-0987(02)00219-1

25. Lipinski CA, Lombardo F, Dominy BW, *et al.*, 2012, Experimental and computational approaches to estimate solubility and permeability in drug discovery and development settings. *Adv Drug Deliv Rev*, 64: 4–17.

https://doi.org/10.1016/j.addr.2012.09.019

26. Huang H, Rong H, Li X, *et al.*, 2008, The crystal structure and identification of NQM1/YGR043C, a transaldolase from *Saccharomyces cerevisiae*. Proteins, 73: 1076–1081.

    https://doi.org/10.1002/prot.22237

27. Wang B, Yang, LP, Zhang XZ, *et al.*, 2009, New insights into the structural characteristics and functional relevance of the human cytochrome P450 2D6 enzyme. *Drug Metab Rev*, 41: 573–643.

    https://doi.org/10.1080/03602530903118729

28. Kakinuma T, Hwang, ST, 2006, Chemokines, chemokine receptors, and cancer metastasis. *J. Leukoc Biol*, 79: 639–651.

    https://doi.org/10.1189/jlb.1105633

29. McEwan IJ, 2009, Nuclear receptors: One big family. *Methods Mol Biol*, 505: 3–18.

    https://doi.org/10.1007/978-1-60327-575-0_1

30. Schwab A, Fabian A, Hanley PJ, *et al.*, 2012, Role of ion channels and transporters in cell migration. *Physiol Rev*, 92: 1865–1913.

    https://doi.org/10.1152/physrev.00018.2011

31. Copeland RA, 2013, Evaluation of Enzyme Inhibitors in Drug Discovery: A Guide for Medicinal Chemists and Pharmacologists. United States: John Wiley & Sons.

32. Leung D, Abbenante G, Fairlie DP, 2000, Protease inhibitors: Current status and future prospects. *J Med Chem*, 43: 305–341.

    https://doi.org/10.1021/jm990412m

33. Barker BS, Young GT, Soubrane CH, *et al.*, 2017, Ion channels. In: Conn's Translational Neuroscience. 1st ed. London: Elsevier Academic Press, p11–43.

    https://doi.org/10.1016/B978-0-12-802381-5.00002-6

34. Ma FH, Li C, Liu YL, 2020, Mimicking molecular chaperones to regulate protein folding. *Adv Mater*, 32: e1805945.

    https://doi.org/10.1002/adma.201805945

35. Savojardo C, Manfredi M, Martelli PL, *et al.*, 2021, Solvent accessibility of residues undergoing pathogenic variations in humans: From protein structures to protein sequences. *Front Mol Biosci*, 7: 626363.

    https://doi.org/10.3389/fmolb.2020.626363

36. Gromiha MM, Ahmad S, 2005, Role of solvent accessibility in structure based drug design. *Curr Comput Aided Drug Des*, 1: 223–235.